interaction associated with the solvent effect. Unfortunately, the detailed nature of this effect cannot yet be specified.

Infrared Spectra

The band centered at *ca.* 837 cm^{-1} in both the PMNB and DNB split into three bands in the labeled materials. The assignment of this absorption band to a molecular vibration has been the subject of a continuing controversy. It has been assigned both to a C–NO_2 stretching motion[24,25,39-41] and to the –NO_2 symmetric deformation.[42,43] Since one would expect that a C–N stretching frequency would be perturbed only slightly by isotopic oxygen substitution (see calculations by Pinchas, *et al.*[42]), our observations that these splittings are of the same magnitude as those observed for the N–O stretching bands support the latter assignment.

(39) K. Nakamura and M. Hasimoto, Proceedings of the International Symposium Molecular on Structure and Spectrometry, Tokyo, 1962, p A104-1.
(40) J. Green, W. Kynaston, and A. Lindsey, *Spectrochim. Acta*, 17, 486 (1961).
(41) H. Shurvell, J. Faniran, E. Symons, and E. Buncell, *Can. J. Chem.*, **45**, 117 (1967).
(42) S. Pinchas, D. Samuel, and B. L. Silver, *Spectrochim. Acta*, **20**, 179 (1964).
(43) V. Farmer, *ibid.*, **23A**, 728 (1967).

Synthesis of Enriched DNB

It is of interest to consider briefly the mechanism of the reaction of NO_2 with *p*-nitrosonitrobenzene. Two distinctly different mechanisms can be formulated: (a) transfer of an oxygen atom from NO_2 to the nitroso group (with or without subsequent oxygen exchange); (b) displacement of the nitroso group by NO_2. The former necessarily leads to a dilution of the isotopic enrichment while the latter leads to no isotope dilution. Including the dilution of enriched oxygen gas with natural NO, and assuming statistical distribution of isotopes, we calculate that 22.5 mole % of the NO_2 was present as $N^{16}O^{17}O$ and 24.8 mole % as $N^{16}O^{18}O$. Mass spectrometric analysis of the DNB finds 23.2 mole % containing one ^{17}O (mass 169) and 25.8 mole % containing one ^{18}O (mass 170), in excellent agreement with the results anticipated for path b.

Acknowledgments. The authors gratefully acknowledge support for this research from the National Science Foundation through Grant GP-4906 as well as through Grant GP-1687 for partial support for purchase of the esr spectrometer. We thank Professor F. W. McLafferty for the mass spectrometric analysis of the enriched dinitrobenzene and Professor Patricia A. Clark for making available to us the results of her CNDO calculations.

Electron Nuclear Double Resonance in Solutions. Spin Densities in Triarylmethyl Radicals

A. H. Maki,[1a] R. D. Allendoerfer,[1a] J. C. Danner,[1a] and R. T. Keys[1b]

Contribution from the Department of Chemistry, University of California, Riverside, California 92502, and California State College, Los Angeles, California 90032. *Received February 10, 1968*

Abstract: Electron nuclear double resonance (ENDOR) and electron paramagnetic resonance (epr) spectra have been obtained of a series of four triarylmethyl radicals [triphenylmethyl, *p*-biphenylyldiphenylmethyl, bis-(*p*-biphenylyl)phenylmethyl, and tris(*p*-biphenylyl)methyl] in solution. The hyperfine coupling constants, obtained directly from the ENDOR spectra, were assigned to specific protons with the aid of observed and calculated epr spectra. The experimental spin density distributions in the π systems are compared to those from a Hückel molecular orbital calculation including McLachlan's perturbation correction.

Electron nuclear double resonance (ENDOR) was first introduced by Feher in 1956 for the study of paramagnetic defects in solids.[2] By means of this technique, nuclear spin transitions may be detected by their effects on the electron paramagnetic resonance (epr) signal. ENDOR thus has become especially useful for investigation of the energy levels of nuclei coupled to unpaired electrons. Until recently, the technique has been limited to investigations in single crystals at or near 4°K. In 1963, Cederquist[3] reported detection of ENDOR signals in alkali metal ammonia solutions in the liquid phase. The nuclear Zeeman transitions which were detected (^{14}N, ^{15}N, ^{1}H, and ^{23}Na) each occurred at essentially its unperturbed Larmor frequency, since the hyperfine coupling with the electron spin is averaged out. In 1964, Hyde and Maki[4] reported the first successful ENDOR measurement of an organic radical in liquid solution in which the bridgehead proton and ring proton nuclear resonance transitions of Coppinger's radical[5] were detected. Later, this work was continued by Hyde,[6] who, using improved instrumentation, was able to observe the weaker *t*-butyl proton ENDOR of Coppinger's radical. Hyde also observed ENDOR of several other repre-

(1) (a) University of California; (b) California State College; National Institutes of Health Special Fellow, 1966–1967, on sabbatical leave at the University of California at Riverside.
(2) G. Feher, *Phys. Rev.*, **103**, 834 (1956).
(3) A. Cederquist, Ph.D. Thesis, Washington University, St. Louis, Mo., 1963.
(4) J. S. Hyde and A. H. Maki, *J. Chem. Phys.*, **40**, 3117 (1964).
(5) G. M. Coppinger, *J. Am. Chem. Soc.*, **79**, 501 (1957).
(6) J. S. Hyde, *J. Chem. Phys.*, **43**, 1806 (1965).

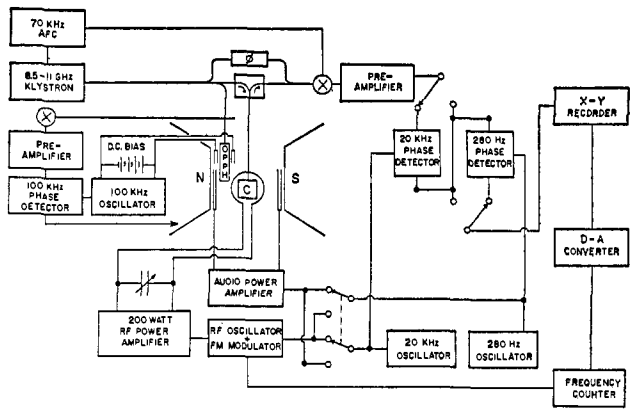

Figure 1. Block diagram of ENDOR spectrometer.

sentative organic free radicals in solution. The power of the ENDOR technique when applied to organic free radicals in solutions is amply demonstrated by the complete analysis of the hyperfine coupling constants of triphenylphenoxyl,[7] and the observation of conformational changes in the hyperfine couplings of (2-methylenethiomethyl)triphenylmethyl.[8] The essential feature necessary for observation of ENDOR in liquids is the use of large nuclear radiofrequency field intensities in order that nuclear spin transitions may be induced in times comparable with electron spin-lattice relaxation times. For free radicals in solution, these are typically 10^{-5}–10^{-6} sec. A theory of ENDOR in liquids has been developed by Freed and coworkers in a series of recent papers.[9-11]

In this communication, we report the ENDOR spectra of a series of triarylmethyl radicals obtained with a spectrometer which is considerably modified from those previously employed.[4,6] The radicals investigated are the series: triphenylmethyl (Ph_3C), (*p*-biphenylyl)diphenylmethyl (Ph_2BC), bis(*p*-biphenylyl)phenylmethyl (PhB_2C), and tris(*p*-biphenylyl)methyl (B_3C). Our interest in these radicals has been directed to an accurate measurement of isotropic proton hyperfine coupling constants and their assignment to the proper ring protons. The use of ENDOR on these radicals is a natural choice due to the numerous small coupling constants and the resulting complicated and poorly resolved hyperfine patterns of their epr spectra. Although ENDOR of solutions can yield the magnitudes of the isotropic coupling constants with great accuracy, little is known, as yet, about the relationship of the intensity of an ENDOR signal and the number of equivalent protons giving rise to it. In this work, therefore, we use a combination of ENDOR, epr, and computer simulation of epr hyperfine patterns to arrive at an accurate determination of the relevant coupling constants with their assignments.

The triphenylmethyl radical has been investigated thoroughly by epr and the assignment of coupling constants given by Chesnut and Sloan,[12] but the other radicals of the series investigated in this paper have not been assigned previously, probably due to the extreme complexity of their hyperfine patterns.

Experimental Section

Instrumentation. The ENDOR spectrometer differs from that described in previous work[4,6] in several respects. Primarily, a continuous rather than a pulsed radiofrequency magnetic field is used to induce nuclear transitions. No gating circuits are thus required. A block diagram of the spectrometer is given in Figure 1.

The microwave section of the spectrometer is constructed from conventional components. The microwave frequency is locked to that of the resonant cavity by means of an ac feedback loop operating at 70 kHz. Part of the microwave power is coupled into a helix containing a diphenylpicrylhydrazyl (DPPH) sample. The helix is equipped with a set of Helmholtz coils used for magnetic field modulation at 100 kHz and for setting up a dc bias field. The derivative DPPH epr signal is phase detected to provide an error signal which is applied to the Varian V-2200A power supply driving the 6-in. electromagnet. The field is thus locked to the frequency of the klystron, since the DPPH remains always at resonance. Once the biasing field is set at the required value to obtain the epr signal of a particular hyperfine line of the free radical in the cavity, severe drifting of the resonant frequency due to radiofrequency heating of the cavity will not cause the spectrometer to drift off the resonance. The radical in the cavity must have a *g* value quite close to that of DPPH in order that the field-frequency locking is effective. The radiofrequency oscillator may be frequency modulated by means of an external audio voltage source. The frequency modulated radiofrequency is amplified to a level of 200 W by means of an Instruments for Industry, Inc. Model 404 broad-band distributed amplifier. The radiofrequency is applied to a tank circuit consisting of a single turn coil about the microwave cavity in parallel with a variable vacuum capacitor. In sweeping the radiofrequency, only tuning of the variable capacitor is required since the passband of the amplifier lies between 250 kHz and 220 MHz. The spectrometer employs a cylindrical TE_{011} cavity having a wire wound cylindrical body, the endplates forming part of the single turn radiofrequency loop, as described previously.[6] Excessive heating of the cavity structure is avoided, however, by making the end plates hollow and circulating cooling water through them. Forced-air cooling of the tank circuit also is used. The cavity is provided with 1-in. diameter stacks in order to accommodate large samples when nonlossy solvents are used.[13]

The spectrometer employs two modulation frequencies, one for Zeeman modulation of the magnetic field and the other for frequency modulation of the radiofrequency. Referring to Figure 1 it is seen that the spectrometer can be used to obtain epr spectra at Zeeman modulation frequencies of 280 Hz or 20 kHz, and ENDOR spectra using 280-Hz Zeeman modulation and 20-kHz frequency modulation or ENDOR spectra with an interchange of these frequencies. Although not obvious from the block diagram, second derivative esr spectra also may be obtained by double Zeeman modulation. If the deviation of the frequency modulation is set smaller than the line width of the nuclear resonance, the ENDOR signal occurs as the first derivative of the epr enhancement. The display thus is similar to that produced by the "differential pulse" technique described by Hyde,[6] although we use a continuous source of radiofrequency power. The 20-kHz component of the ENDOR signal is first amplified and phase detected by a rather broadbanded circuit which passes the 280-Hz amplitude modulation. The latter is subsequently amplified, phase detected, and applied to the *y* axis of an *x*–*y* recorder. The radiofrequency oscillator is monitored by a frequency counter which drives a digital-to-analog converter, the output of which drives the *x* axis of the recorder. Frequency-swept ENDOR spectra thus are displayed on a scale which is linear in frequency.

In these experiments, the samples, dissolved in toluene, were contained in 8-mm o.d. quartz tubes. Temperature control was achieved by passing chilled nitrogen gas through a Styrofoam dewar surrounding the sample. Temperatures used were between −60 and −80° and were adjusted for the most intense ENDOR spectra. The epr spectra were obtained with a conventional Varian V-4502 spectrometer with a 9-in. electromagnet driven by a Varian Mark II Fieldial power supply. The temperature was maintained by cooled nitrogen gas flow at a value which gave the maximum resolution of the hyperfine structure.

(7) J. S. Hyde, *J. Phys. Chem.*, 71, 68 (1967).
(8) J. S. Hyde, R. Breslow, and C. DeBoer, *J. Am. Chem. Soc.*, 88, 4763 (1966).
(9) J. S. Freed, *J. Chem. Phys.*, 43, 2312 (1965).
(10) J. S. Freed, *J. Phys. Chem.*, 71, 38 (1967).
(11) J. S. Freed, D. S. Leniart, and J. S. Hyde, *J. Chem. Phys.*, 47, 2762 (1967).
(12) D. B. Chesnut and G. J. Sloan, *ibid.*, 33, 637 (1960).
(13) A. Carrington and J. S. Hyde, private communication.

Computer Simulation of Esr Spectra. A program which has been described previously[14] was modified for use with a Cal-Comp Plotter, Model 470. The program calculates the expected esr hyperfine pattern to first order in the hyperfine interaction, given the hyperfine coupling constants, numbers of equivalent nuclei, line shape, and width. The computations were done on an IBM Model 7040 computer.

Preparation of the Radicals. The radicals were prepared by treating the appropriate halide with granular silver[15] in toluene within a Vacuum Atmospheres Corp. "Dri-train" drybox under nitrogen atmosphere. The solution was shaken for 15 min and transferred to the sample tube. No attempt was made to isolate the hydrocarbon dimer. The tube was then placed on a vacuum line, degassed, and sealed off. The radicals were stored in the dark and showed little appreciable decay after 2 or 3 weeks except for PhB_2C, which gave evidence of decomposition after 2 days. On the basis of complete dissociation, the starting concentration of all of the radical solutions was 0.003 *M*. The samples were diluted in some cases by distillation of solvent within the apparatus after seal-off in order to optimize the conditions for observing ENDOR.

The three biphenyl-substituted methyl chlorides all were prepared using the original procedure of Schlenk.[16] In this method the carbinol was prepared by the appropriate Grignard reaction, purified, and converted to the chloride with acetyl chloride. Column chromatography over acid-washed alumina (Reagent grade from Merck & Co., Inc.) as well as recrystallization was used to purify the carbinols. Over-all yields of the chlorides, while low (*ca.* 10%), were adequate to give ample samples for theses tudies. The starting materials used in the preparation of each chloride synthesized are given below. All melting points are uncorrected.

Triphenylmethyl chloride was donated by Professor J. Casanova (California State College, Los Angeles). It had been recrystallized from ligroin and was used as received.

[Biphenylyl-(4)]diphenylmethyl chloride had a melting point of 147–148° (lit.[16] 147.5°). The carbinol which melted at 112–114° (lit.[17] 112–113°)[17] was prepared from the methyl ester of 4-biphenylylcarboxylic acid and iodobenzene. The ester had been made from the acid which was obtained from the Aldrich Chemical Co. The acid was twice recrystallized from toluene before use. The iodobenzene was obtained from Matheson Coleman and Bell and was dried over molecular sieves (Linde Type 4A) prior to use.

Di[biphenylyl-(4)]phenylmethyl chloride had a melting point of 128–131° (lit.[16] 131.5°). The carbinol melted at 151–152° (lit.[16] 150°) and had been prepared from 4,4′-diphenylbenzophenone and iodobenzene. The ketone, synthesized from phosgene and biphenyl,[18] was purified by repeated recrystallizations and column chromatography using warm xylene as the eluent.

Tri[biphenylyl-(4)]methyl chloride had a melting point of 195–198° (lit.[16] 195°). The carbinol melted at 194–202° (lit.[16] 207–208°). It was synthesized from 4,4′-diphenylbenzophenone and 4-iodobiphenyl. The 4-iodobiphenyl was purchased from Eastman Organic Chemicals. It was recrystallized twice and zone refined prior to use.

Detection of ENDOR

The field homogeneity of the ENDOR spectrometer was not sufficient to obtain well-resolved epr spectra when operated in that mode, except in the case of triphenylmethyl which has relatively few (196) hyperfine lines. No attempt was made in these experiments to lock the spectrometer onto a single hyperfine line. Rather, the Zeeman modulation amplitude was adjusted to give the maximum possible peak-to-peak derivative amplitude for the single hyperfine envelope. For these radicals, the optimum modulation amplitude was 5 to 10 G peak-to-peak. By means of this technique the field-stability requirement for observing ENDOR is reduced, and the field-frequency locking was not used in these measurements. The technique of overmodulating

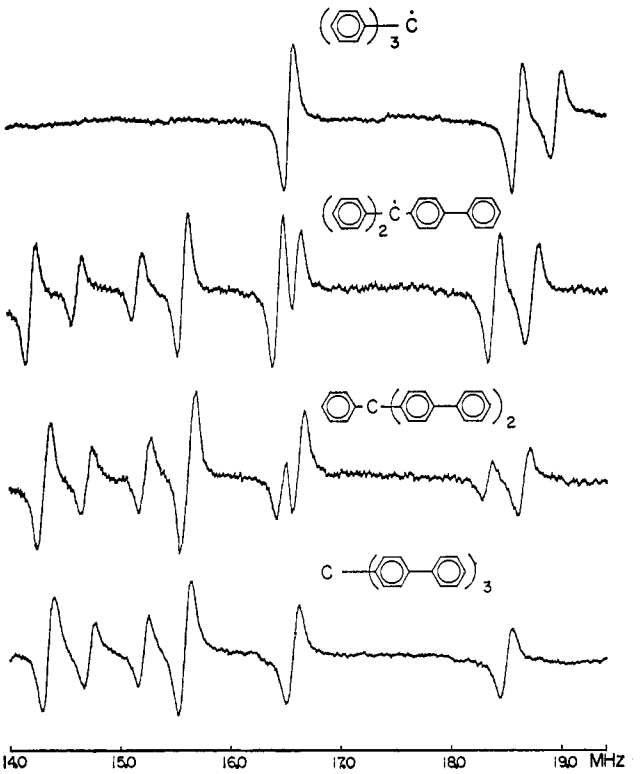

Figure 2. ENDOR spectra of four triarylmethyl radicals in the frequency range 14–19.5 MHz. Proton Larmor frequency is 14.9 MHz in each spectrum.

poorly resolved epr spectra containing a large number of hyperfine lines does not broaden the ENDOR transitions significantly and is known to produce strong ENDOR signals.[6–8] The microwave power level incident on the cavity was varied in each case to give the maximum ENDOR signals. The optimum power level was close to that just sufficient to give the maximum epr signal. ENDOR transitions were observed under these conditions *provided the Zeeman modulation was done at the low frequency* (280 Hz). Zeeman modulation of comparable amplitude at 20 KHz produced no detectable ENDOR signals. We have observed, however, that if the modulation amplitude is reduced to a small value, comparable to the width of a well-resolved epr line (~0.1 G), both Zeeman modulation frequencies appear to work equally well for strongly coupled protons, but the higher frequency discriminates against ENDOR of weakly coupled protons. This effect, which is probably connected with the velocity at which the Zeeman field traverses a spin packet, will be reported on more fully in a future communication. The power level of the radiofrequency in the tank circuit was maintained near the maximum output of the amplifier (200 W) although its level probably varied significantly over the frequency range employed due to variation in the matching of the tank circuit with the amplifier. ENDOR spectra were recorded over the frequency range 14–19.5 MHz, and are shown in Figure 2. The ENDOR spectra have an approximate center of symmetry occurring at the unshifted proton Zeeman frequency in the fixed field of the experiment. The lack of exact symmetry can be explained by second-order frequency shifts as described in the following section. For each of the spectra the center frequency is close to 14.9 MHz. The frequency

(14) E. W. Stone and A. H. Maki, *J. Chem. Phys.*, **38**, 1999 (1963).
(15) G. M. Schwab and E. Agallidis, *Z. Physik. Chem.*, 41B, 59 (1938).
(16) W. Schlenk, *Ann. Chem.*, **368**, 295 (1909).
(17) D. B. Clapp and A. A. Morton, *J. Am. Chem. Soc.*, **59**, 2074 (1937).
(18) M. P. Adam, *Ann. Chim. Phys.*, **6**, 15, 258 (1888).

was determined by averaging of frequencies of the two central pairs of mirror-image ENDOR lines of the lowest three spectra of Figure 2. All six expected lines of triphenylmethyl were measured, although only the three highest frequency lines are shown in Figure 2.

Interpretation of the ENDOR Spectra

The Zeeman energy levels of a free radical in solution in an applied magnetic field **B** are given by the eigenvalues of the Hamiltonian, $\mathcal{H}_0$, where

$$\hbar\mathcal{H}_0 = g_s|\beta|\mathbf{B}\cdot\mathbf{S} - \hbar\mathbf{B}\cdot\left(\sum_i \gamma_i \mathbf{I}_i\right) - \gamma_e\mathbf{S}\cdot\left(\sum_i a_i\mathbf{I}_i\right) \quad (1)$$

in which the index i labels nuclei with contact hyperfine coupling constant a_i (expressed in gauss), spin operator $\mathbf{I}_i$, and magnetogyric ratio γ_i. The quantities β, g_s, **S**, and γ_e are the Bohr magneton, solution g value, spin operator, and magnetogyric ratio of the electron, respectively.

A free-radical frequently has identical nuclei which have equivalent coupling constants because of symmetry, rapid averaging of inequivalent positions, etc. In this case, as was shown by Fessenden,[19] it is appropriate to group identical nuclei with the same coupling constant together, and to couple the individual nuclear angular momenta within the groups.[20] Thus, if κ, λ, $\cdots$, are used to label the groups of nuclei with coupling constants a_κ, a_λ, $\cdots$, the Hamiltonian (eq 1) becomes

$$\hbar\mathcal{H}_0 = g_s|\beta|\mathbf{B}\cdot\mathbf{S} - (\hbar\gamma_\kappa\mathbf{B} + \gamma_e a_\kappa\mathbf{S})\cdot\mathbf{K} - (\hbar\gamma_\lambda\mathbf{B} + \gamma_e a_\lambda\mathbf{S})\cdot\mathbf{L} - \cdots \quad (2)$$

where $\mathbf{K} = \Sigma_{i\,\mathrm{in}\,\kappa}\mathbf{I}_i$, $\mathbf{L} = \Sigma_{j\,\mathrm{in}\,\lambda}\mathbf{I}_j$, ... are the resultant group angular momenta. We shall consider the $S = {}^1/_2$ and $I = {}^1/_2$ case with each interacting nucleus a proton. This represents the radicals which we have measured. The energy levels of the Hamiltonian (eq 2) are given to second order in perturbation theory by

$$E^{(2)} = g_s|\beta|Bm_s - \hbar[(\gamma_n B + \gamma_e a_\kappa m_s)M_K + (\gamma_n B + \gamma_e a_\lambda m_s)M_L + \cdots] + \frac{\hbar^2 m_s \gamma_e^2}{2g_s|\beta|B}\{a_\kappa^2[K(K+1) - M_K(M_K + 2m_s)] + a_\lambda^2[L(L+1) - M_L(M_L + 2m_s)] + \cdots\} \quad (3)$$

In eq 3 m_s is the quantum number for the field component of the electron spin, **s**, while M_K, M_L, $\cdots$, are the quantum numbers for the components of the nuclear group momenta, **K**, **L**, $\cdots$, along the direction of the field. The allowed nuclear transitions which give rise to the ENDOR enhancements of the epr signal have the selection rules $\Delta K = \Delta L = \cdots = 0$, $\Delta m_s = 0$, and $\Delta M_K = \pm 1$ for ENDOR of κ protons, $\Delta M_L = \pm 1$ for ENDOR of λ protons, etc.

Thus to second order in perturbation theory, eq 3 yields the following energy differences between the M_K and $M_K + 1$ levels.

$$E^{(2)}(M_K) - E^{(2)}(M_K + 1) = \hbar(\gamma_n B + \gamma_e a_\kappa m_s) + \frac{\hbar^2\gamma_e^2 m_s a_\kappa^2}{g_s|\beta|B}(M_K + m_s + {}^1/_2) \quad (4)$$

To first order, the nuclear transitions occur at the frequencies

$$\omega_\kappa = \gamma_n B + \gamma_e a_\kappa m_s$$
$$\omega_\lambda = \gamma_n B + \gamma_e a_\lambda m_s$$
$$\cdots$$
$$\cdots \quad (5)$$

Each group of equivalent protons, to first order, gives ENDOR signals at two frequencies, depending on the quantum number m_s. Thus, one of these transitions is associated with the upper electron Zeeman level ($m_s = +{}^1/_2$) and one with the lower ($m_s = -{}^1/_2$). Both of these transitions are observed in practice, if their frequencies lie within the effective range of the radio-frequency circuits.

The second-order frequency shifts for the nuclear transitions obtained from eq 4 is

$$\omega^{(2)}{}_{M_K \to M_K+1} = \frac{m_s\omega_\kappa^2}{\omega_e}(M_K + m_s + {}^1/_2) \quad (6)$$

where $\omega_e = g_s|\beta|B/\hbar$ is the electron Larmor frequency. Since the Zeeman modulation of the magnetic field in our experiments was wide enough to cover most of the hyperfine structure of the epr spectrum, contributions to the ENDOR enhancement of the κ protons must have arisen from a distribution of M_K states. For the purpose of estimating the second-order shift of the ENDOR lines, we will assume that in the experiment (a) *all* values of M_K contribute to the signal, (b) the contribution to the ENDOR intensity of a given state K, M_K is proportional to the nuclear magnetic transition moment $\langle K_+K_-\rangle$, or $\langle K_-K_+\rangle$, and (c) the shift of the ENDOR line is given by the average shift of the individual M_K lines weighted by the nuclear transition moments. Under these conditions, the mean second-order shifts for the ENDOR signals for $\Delta M_K = +1$ and $\Delta M_K = -1$ transitions within the manifold of constant K, are given by the equations

$$\omega^{(2)}{}_\pm = \frac{m_s\omega_\kappa^2}{\omega_e}\left(m_s \pm {}^1/_2 + \frac{\mathrm{tr}\langle M_K K_\mp K_\pm\rangle}{\mathrm{tr}\langle K_\mp K_\pm\rangle}\right) \quad (7)$$

Upon evaluation of the traces, eq 7 leads to the same simple expression for the mean second-order shift of the ENDOR lines

$$\omega^{(2)}{}_\pm = \omega_\kappa^2/4\omega_e \quad (8)$$

The result is independent of the m_s value and therefore predicts that each ENDOR line for a particular class of protons is shifted to higher frequencies by the same amount. The spacing between the line centers of gravity is thus equal to the hyperfine frequency, ω_κ, to second order in perturbation theory, while their average value is shifted by $\omega_\kappa^2/4\omega_e$ from the Larmor frequency of a free proton. The accuracy of the ENDOR transitions in our experiments was limited by the instability of the magnetic field to about ±4 kHz and is not sufficient to detect the second-order shift predicted by eq 8. A second-order frequency shift of only 1.6 kHz is predicted for the strongly coupled protons of Ph_3C.

Assignment of Hyperfine Splitting Constants

While the ENDOR spectrum gives very precise values of the hyperfine splitting constants, it yields

(19) R. W. Fessenden, *J. Chem. Phys.*, 37, 747 (1962).
(20) M. K. Banerjee, T. P. Das, and A. K. Saha, *Proc. Roy. Soc.* (London), A226, 490 (1954).

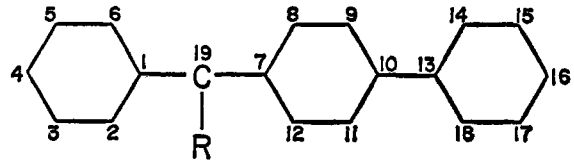

Figure 3. Numbering of carbon positions in triarylmethyl radicals

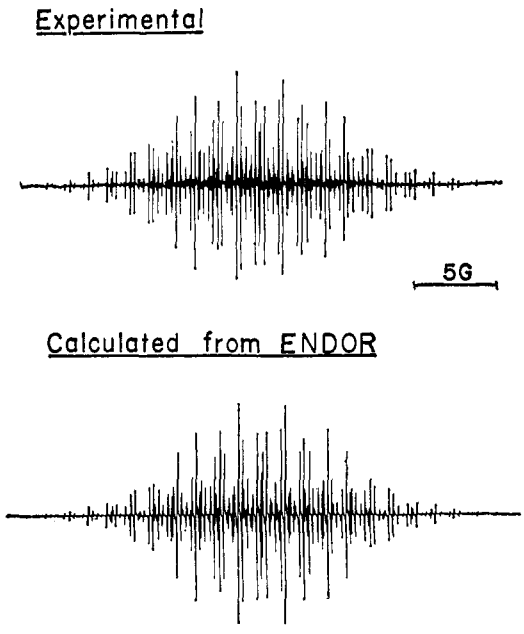

Figure 4. Comparison of experimental and calculated epr spectra of triphenylmethyl. Coupling constants were obtained from ENDOR. Line shape is Gaussian, with a line width (peak to peak) of 50 mG.

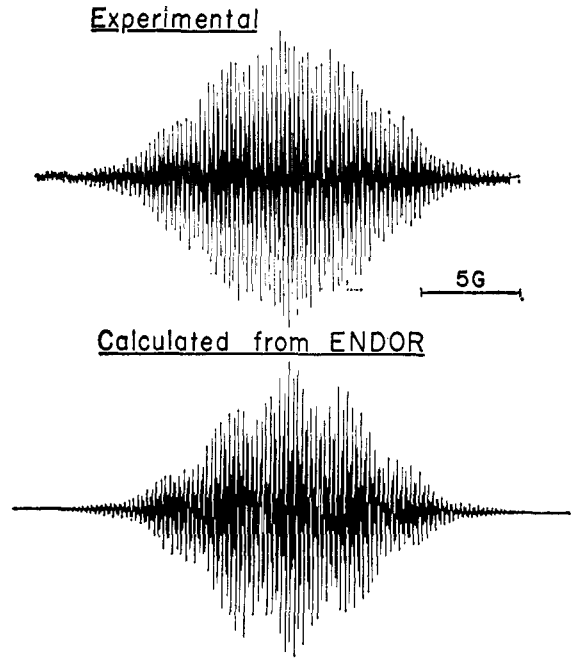

Figure 5. Comparison of experimental and calculated epr spectra of tris(*p*-biphenylyl)methyl. Coupling constants were obtained from ENDOR and assigned as in the text. Calculated line shape is Gaussian with a peak to peak line width of 60 mG.

relatively little information about the assignment of these splittings to specific positions in the molecule. Because of the difficulties associated with interpreting the effects of temperature, microwave power, and Zeeman modulation velocity, the relative intensities of peaks in an ENDOR spectrum do not correspond, in general, to the relative numbers of equivalent protons responsible for the enhancement. Over very small frequency ranges for similar types of protons, however, the effects mentioned above seem to be less important and peak amplitudes are roughly proportional to the number of protons. However, even in this case the agreement is not precise and this criterion for assignment should be used with a large grain of salt.

The types of carbon atoms in the four radicals studied, Ph_3C, Ph_2BC, PhB_2C, and B_3C can be numbered in general as in Figure 3.

The assignment of the three splittings in Ph_3C is straightforward and has been given previously.[6] Comparison of the experimental spectrum and the epr spectra computed for the various possible assignments gives unambiguously that $|a_4| > |a_2| > |a_3|$. In all our assignments we assume that the proton coupling constants of unstarred positions (starring the methyl carbon) are smaller than those of corresponding starred positions within the same phenyl ring. The ENDOR intensity ratio for line 2 to line 3 (counting toward higher frequencies from the center of the ENDOR spectrum) is 1.6:1 rather than the predicted 2:1. Figure 4 shows an experimental epr spectrum and one computed from the ENDOR splitting constants as assigned above.

Adding a second phenyl ring in the *para* position is expected to have little more than a dilution effect on the spin density distribution of the inner ring so that the largest splitting constant in B_3C can be assigned to position 8 by analogy with Ph_3C and similarly the second largest to position 9. Thus the remaining two small splittings in B_3C must be from protons of the outer phenyl ring, positions 14, 15, and 16. Simple molecular-orbital or valence-bond treatments of the spin density distribution in the outer ring give $|a_{14}| \cong |a_{16}| > |a_{15}|$. Thus, we assign the smallest splitting to position 15, and the other line must be due to a_{14} and a_{16}. The difference between a_{14} and a_{16} must be considerably less than 100 kHz since their ENDOR enhancements are not resolved. The ENDOR intensity ratio is 3.9:2 rather than the predicted 3:2. Figure 5 shows the experimental epr spectrum and one computed from the ENDOR splitting constants.

From comparisons with Ph_3C and B_3C, the ENDOR lines from Ph_2BC and PhB_2C may be grouped into three sets. The innermost pair of lines must be assigned to a_{14}, a_{15}, and a_{16}. The intermediate pair of lines must be assigned to a_3 and a_9, and the outermost pair must be due to a_2, a_4, and a_8. The assignment $|a_{14}| \cong |a_{16}| > |a_{15}|$ is made as for B_3C. Computations of epr spectra were made for each choice of a_3 and a_9 for both compounds and in each case $|a_9| > |a_3|$ clearly gave a superior fit to the experimental epr spectrum. This result is in accord with the molecular-orbital calculations discussed below and the ENDOR intensities. For Ph_2BC the experimental intensity ratio for this pair is 2.0:1 where 2:1 is expected, and for PhB_2C the measured ratio is 1.1:2 where 1:2 is expected. The remaining three coupling constants are assigned to the two outermost ENDOR

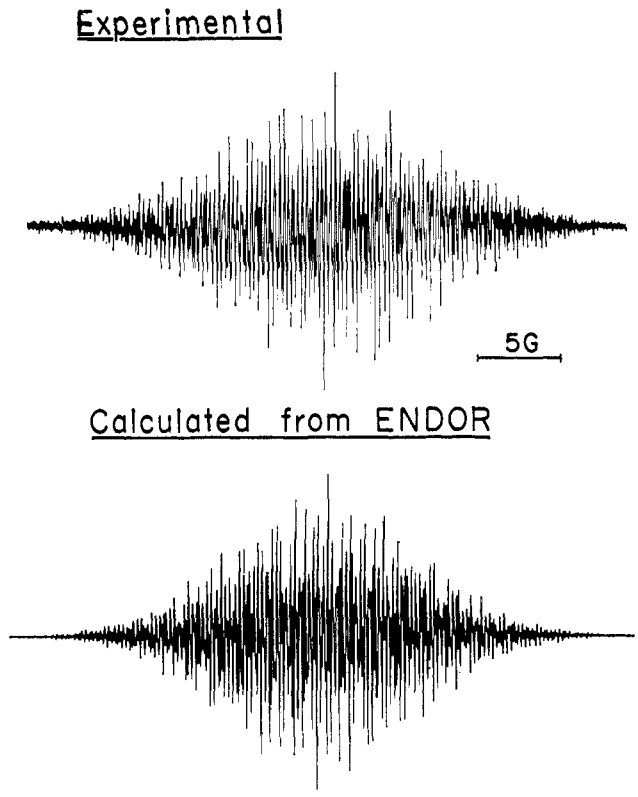

Figure 6. Comparison of experimental and calculated epr spectra of (*p*-biphenylyl)diphenylmethyl. Coupling constants were obtained from ENDOR and assigned as described in the text. Calculated line shape is Gaussian with a peak to peak line width of 60 mG.

lines according to the following considerations. It is unreasonable to expect that the *ortho/para* spin density ratio in a phenyl ring should change appreciably as the other phenyl rings in the molecule are substituted. Hückel molecular-orbital theory, for example, predicts that this ratio is always unity. Thus we assign $|a_4| > |a_2|$ in both Ph_2BC and PhB_2C by analogy with Ph_3C. That $a_4 \cong a_8$ rather than $a_2 \cong a_8$ can be seen clearly from comparison of the computed and experimental epr spectra. The 100-kHz line width again puts a 100-kHz upper limit on this equivalence. The ENDOR intensity ratio of the outer two lines for Ph_2BC is 1.4:1 where 1:1 is expected, and for PhB_2C it is 2.8:5 where 2:5 is predicted by the assignment above. On the other hand, the assignment $a_2 \cong a_8$ predicts the intensity ratios of the outer lines to be 3:1 and 6:1 in Ph_2BC and PhB_2C, respectively, in complete disagreement with the observed intensities. Figures 6 and 7 show the experimental and computed epr spectra for Ph_2BC and PhB_2C, respectively.

None of the experimental epr spectra of the more complex radicals agrees perfectly with the computed ones. There are several possible reasons for this. One is that the experimental spectra were slightly saturated in order to obtain sufficient signal to noise in the wings. This makes the wings relatively more intense and the lines in the center somewhat broader and therefore less well resolved. Also, the phase of the 100-kHz reference signal on the Varian epr spectrometer used to obtain these spectra was adjusted for *maximum resolution* and not *maximum signal intensity*. The 100-kHz side bands can be altered in this manner so that apparent peak-to-peak line widths of 50 mG, but peculiar line shapes, are obtained. A Gaussian line

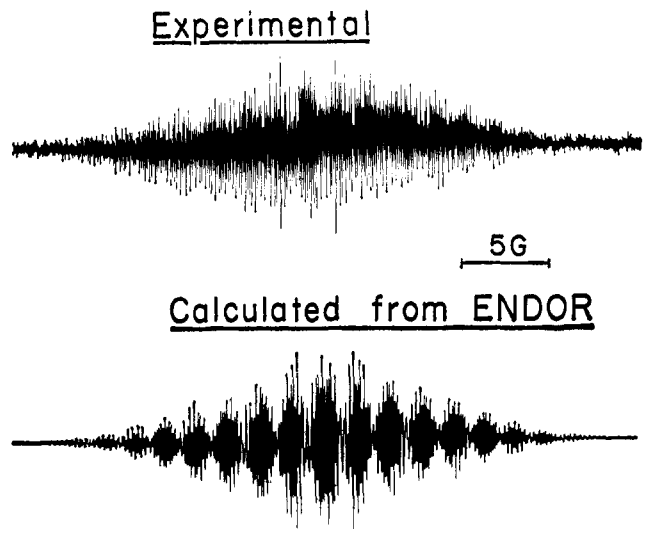

Figure 7. Comparison of experimental and calculated epr spectra of bis(*p*-biphenylyl)phenylmethyl. Coupling constants were obtained from ENDOR and assigned as described in the text. Calculated line shape s Gaussian with a peak to peak line width of 60 mG.

shape was chosen for the computed spectra, which appears to give a better fit than a Lorentzian line shape but is not necessarily the best choice. As noted earlier, solutions of PhB_2C were not particularly stable, and the epr spectrum may contain lines due to impurities.

The assignments made as described above are given in Table I, along with the computed values in gauss. A discussion of the MO calculations is given in the next section.

Calculation of Spin Densities

There are in the literature a wide range of approaches to the calculation of spin densities in π-type free radicals. Recently, these methods were reviewed[21] and their respective predicted spin density distributions compared with spin densities inferred from experiment. While some form of electron correlation is required in order to produce negative spin densities, it has turned out that the McLachlan perturbation approximation[22] to self-consistent field theory produced results as satisfactory as the later, more elaborate methods. For this reason, we have chosen the McLachlan approximation to calculate spin densities. It should be noted that the calculations[21,22] do not predict the correct ordering of *ortho* and *para* coupling constants for triphenylmethyl (*i.e.*, experimentally $a_p > a_o$).[12] The same problem occurs with benzyl which has been subjected to an exhaustive array of calculations.[23] For this reason, our objective was to look for trends in the coupling constants in this series of radicals and to try to fit the spin density variations on corresponding atoms in the different rings. Since all of the rings have "*ortho*" protons, we have chosen these to compare with the experimental data. In making such a comparison, one has to assume a value for Q, the McConnell proportionality constant.[24] $Q = -27$ G[25] was used. The spin densities do not depend strongly on the choice of λ, the semiempirical constant in the

(21) G. G. Hall and A. T. Amos, *Advan. Atomic Mol. Phys.*, 1, 36, (1965).
(22) A. D. McLachlan, *Mol. Phys.*, 3, 233 (1960).
(23) A. Carrington and I. C. P. Smith, *ibid.*, 9, 137 (1965).
(24) H. M. McConnell, *J. Chem. Phys.*, 24, 632 (1956).
(25) L. C. Snyder and A. T. Amos, *ibid.*, 42, 3670 (1965); M. Karplus and G. K. Fraenkel, *ibid.*, 35, 1312 (1961).

Table I. Experimental and Calculated Coupling Constants of Triarylmethyl Radicals[a]

Compound	$-a_2$	$-a_3$	$-a_4$	$-a_8$	$-a_9$	$-a_{14}$	$-a_{15}$	$-a_{16}$
Ph_3C								
ENDOR	2.609[b]	1.143	2.857					
Twisted calcn	2.599[b]	−0.970	2.398					
Planar calcn	2.930	−1.052	2.760					
Ph_2BC								
ENDOR	2.474	1.100	2.715	2.715	1.206	0.487	0.193	0.487
Twisted calcn	2.503	−0.910	2.327	2.703	−1.007	0.465	−0.194	0.430
Planar calcn	2.833	−0.994	2.681	2.784	−1.011	0.642	−0.251	0.604
PhB_2C								
ENDOR	2.377	1.067	2.604	2.604	1.168	0.462	0.185	0.462
Twisted calcn	2.405	−0.856	2.249	2.601	−0.946	0.454	−0.183	0.423
Planar calcn	2.735	−0.941	2.598	2.690	−0.955	0.627	−0.238	0.592
B_3C								
ENDOR				2.499[b]	1.136	0.438[b]	0.174	0.438
Twisted calcn				2.499[b]	−0.891	0.442[b]	−0.172	0.414
Planar calcn				2.596	−0.905	0.610	−0.226	0.579

[a] Experimental values, obtained from the ENDOR frequencies, are expressed in gauss. The uncertainty is approximately ±0.003 G. Only absolute values are known experimentally. Proton positions are given in Figure 3. [b] These are the coupling constants used to fit effective resonance integrals for ring-joining bonds.

McLachlan approximation,[22] and we used a value of 1.2.

In Table I, from the lines labeled "Planar calcn," it can be seen that the assumption of planar radicals and $Q = -27$ G gives poor agreement with the experimental assignments. It has been known since the work of Lewis, *et al.*,[26] that these radicals probably have a "windmill' or "propeller" configuration. While it is impossible to infer an exact angle of ring pitch from epr data,[27] it is reasonable to expect the twist will result in a somewhat lower value of β_{rs} for r and s corresponding to adjacent atoms on different rings. Following Streitwieser,[28] we let $\beta_{rs} = k_{rs}\beta$ and varied the value of k_{rs} for the three different types of ring-linking "β's" until the computed spin densities agreed with the experimental ones obtained using $Q = -27$ G.[29] $k_{1,19} = 0.87$ was determined from the best fit to the Ph_3C data. $k_{7,19} = 0.91$ and $k_{10,13} = 0.88$ were determined from fitting the B_3C data. These values of the k were used without further variation to calculate the coupling constants of Ph_2BC and PhB_2C. The hyperfine splittings computed in this way are given in Table I, on the lines labeled "Twisted calcn."

The low values of β_{rs} required may be rationalized in several ways. If the rings are twisted out of the plane of the molecule, then one might assume $k = \cos\theta$ where θ equals the angle of ring twist. For the k's obtained, θ values of 24–30° would result. The crystal structure of triphenylmethyl perchlorate has been determined recently,[30] and the phenyl rings have been found to be twisted by 31.8° with respect to the average plane of the molecule. It is reasonable, therefore, to expect a similar twisting of the rings of triphenylmethyl radical, though perhaps to a lesser extent. The angle of twist of biphenyl in solution is generally assumed to be about 20°,[31-33] and the ring–ring carbon bond distance of 1.48 Å of biphenyl in the gas phase[34] is significantly longer than the usual aromatic carbon–carbon bond distance of 1.40 Å. Even in the solid state where the rings are flat, the ring–ring carbon bond distance is 1.50 Å,[35] although this lengthening could be due partially to intermolecular interactions, as well as intramolecular ones. Such a lengthening of a bond could also diminish β_{rs} sufficiently to explain the values of k obtained.[28]

The particularly encouraging aspect of the results of the spin-density calculations with reduced inter-ring resonance integrals can be seen from examination of the results for Ph_2BC and PhB_2C in Table I. Whereas the calculation for a planar radical with unaltered inter-ring resonance integrals predicts $|a_2| > |a_8|$, the calculation for a "twisted" radical correctly predicts $|a_8| > |a_2|$. A reasonable prediction of the coupling constants of Ph_3C and B_3C could have been obtained using a value of $Q = -24$ G, but this would not have affected the relationship between a_2 and a_8 in the other radicals. Even with some variation in the choice of Q, some adjustment of the inter-ring resonance integrals is necessary in order to obtain the proper relationship. Also, except for a_4, the p-proton coupling, the calculated coupling constants for the "twisted" radical are seen to be in remarkably good agreement with experiment.

Thus, we can say that the calculations support the suggestion that all of the ring links are twisted, stretched, or some combination thereof.

Acknowledgments. The authors wish to thank Professor F. Heineken of the American University, Beirut, Lebanon, for assistance in the construction of the ENDOR spectrometer and J. S. Hyde of Varian Associates for numerous helpful discussions. We are grateful for the support of this work by the National Science Foundation through Grant GP-6656. We are grateful to the University of California, Riverside Computer Center, for the use of their facilities.

(26) G. N. Lewis, D. Lipkin, and T. T. Magel, *J. Am. Chem. Soc.*, **66**, 1579 (1944).
(27) S. I. Weissman and J. C. Sowden, *ibid.*, **75**, 520 (1953).
(28) A. Streitwieser, Jr., "Molecular Orbital Theory for Organic Chemists," John Wiley and Sons, Inc., New York, N. Y., 1961.
(29) The best values of the β_{rs} depend rather strongly on the choice of Q, and are, as a consequence, somewhat arbitrary.
(30) A. H. Gomes de Mesquita, C. H. MacGillavry, and K. Eriks, *Acta Cryst.*, **18**, 437 (1965).
(31) H. Volz and M. J. Volz de Lecea, *Tetrahedron Letters*, 4675, 4683 (1966).
(32) H. Hart, T. Sulzberg, R. W. Schwendeman, and R. H. Young, *ibid.*, 1337 (1967).
(33) H. Suzuki, *Bull. Chem. Soc. Japan*, **32**, 1340 (1959).
(34) O. Bastiansen, *Acta Chem. Scand.*, **3**, 408 (1949).
(35) A. Gargreaves and S. H. Rizvi, *Acta Cryst.*, **15**, 365 (1962).